# Simulation of Coherent Remission in Planar Disordered Medium

Pablo Jara-Palacios
Physics Department
Missouri University of Science
and Technology
Rolla, MO, USA
pxjdbk@mst.edu

Ho-Chun Lin
Ming Hsieh Department of
Electricall and Computer
Engineering
University of Southern California
Los Angeles, CL, USA
hochunli@usc.edu

Alexey Yamilov
Physics Department
Missouri University of Science
and Technology
Rolla, MO, USA
yamilov@mst.edu

Chia Wei Hsu

Ming Hsieh Department of
Electrical and Computer
Engineering
University of Southern California
Los Angeles, CL, USA
cwhsu@usc.edu

Hui Cao

Department of Applied Physics

Yale University

New Haven, CT, USA
hui.cao@yale.edu

Abstract— Waves remitted from a scattering medium carry information that can be used for non-invasive imaging and sensing. Such techniques are usually limited by a low photon budget. Recent progress in optical wavefront shaping has enabled coherent control with an order-of-magnitude enhancement of remission [1]. This experimental study necessitated increasingly demanding numerical simulations. Extending this line of research requires more sophisticated computational techniques capable of simulating multiple instances of even larger systems. Here, we demonstrate that remission geometry can be efficiently simulated using a novel open-source software package [2] Maxwell's Equations Solver with Thousands of Inputs (MESTI). To verify its numerical performance, several simulations and comparisons with the method used previously are presented. Excellent qualitative and quantitative agreement with previous results is obtained. Additionally, orders of magnitude improvement in the computational performance of MESTI is observed. This opens the path to computational modeling of spectral and temporal remission from large scattering systems.

Keywords—diffusion, disordered media, remission eigenvalues, remission matrix.

### I. INTRODUCTION

There are many practical circumstances where one cannot access the interior of a sample to employ a transmission setup, either because it is not physically possible or desirable, e.g., for in vivo biological systems. In these cases, one is limited to receiving a signal on the same side of the surface from which light impinges. An arrangement where the excitation and collection areas are displaced, c.f. inset in Fig. 1, offers several practical advantages such as an ability to reject strong back-reflections and the possibility of depth-sensitive measurement [1]. This configuration is called remission geometry.

Recently, by taking advantage of the determinism of light propagation in disorder media, wavefront shaping technology enabled a coherent manipulation of light transport between a source and detector [3]. Due to the inherent complexity of the problem, an analytical description of the sample-specific wave field distribution is not feasible, making one rely heavily on the numerical simulations either to test or to verify theoretical or experimental results. This problem demands robust computational approaches capable of simulating extremely large volume  $L^d \gg \ell_t^d \gg \lambda^d$ , where L is the size of system,  $\ell_t$  is the transport mean free path,  $\lambda$  is the wavelength in the medium, and d is the dimensionality of the system.

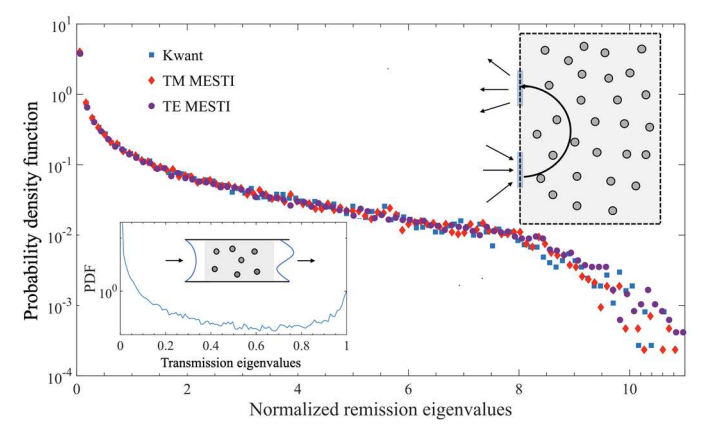


Fig. 1. Agreement between probability density function (PDF) of the remission eigenvalues obtained numerically using Kwant (squares), MESTI/TM (diamonds), and MESTI/TE (circles) methods in 2D slab geometry (upper inset); see text for system parameters. PDF of transmission eigenvalues, the bimodal distribution in the waveguide geometry (lower inset) obtained using MESTI/TE, differs markedly from that for remission [1].

The planar geometry in Ref. [1], see also inset in Fig. 1, allows detection of the wave field inside the scattering region. This eases computational requirements by lowering the dimensionality of the system to d=2, however, the simulation volume (area in 2D) is still large  $\left(\frac{L}{\lambda}\right)^2 \propto 2.5 \times 10^5$ . Previously, we have employed the Kwant [4] simulation package, an opensource software, developed for continuous wave (CW) simulations of the electronic wave transport and, thus, suitable only for modelling the transverse magnetic (TM) polarization of

This work was supported by the National Science Foundation under Grants No. DMR-1905442, DMR-1905465 and OAC-1919789.

the electromagnetic (EM) waves. The experiment, however, involves propagation of the transverse electric (TE) polarized waves. With a suitable choice of the scattering strength in the Kwant simulations, an agreement was obtained by choosing  $\ell_t$ to match the experimental conditions [1]. However, computation requirements, particularly memory usage, were the limiting factors to a more extensive use of the method. Considering the statistical nature of wave propagation in complex media, where simulations must be run for large ensembles of realizations (e.g. disorder configurations, or sufficiently separated frequencies), MESTI's improved computational speed and relaxed memory requirements together with proper treatment of TE polarization and dispersion open the path to extending previous analyses to studies of spectral and temporal properties of the system. Below, we present several tests and verifications of the new method.

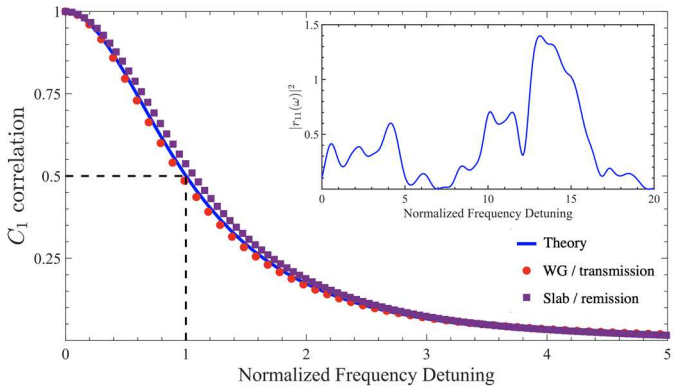


Fig. 2. MESTI/TE simulations. Inset shows an example of frequency dependence of an element of the remission matrix. Frequency correlation function  $\mathcal{C}_1$  found for transmission (waveguide) and remission (slab) are described well by theoretical formula.

## II. RESULTS AND DISCUSSION

We use the MESTI package to perform TM and TE simulations for the planar (2D) for the remission/slab and transmission/waveguide geometries, schematically depicted in insets of Fig. 1. System parameters are chosen similar to those in experiments in Refs. [1,5]: vacuum wavelength  $\lambda_0$  = 1.55  $\mu$ m, effective refractive index  $n_{\rm eff} = 2.85$ , slab size is  $L \times$  $W = 200 \,\mu\text{m} \times 400 \,\mu\text{m}$  and waveguide size is  $50 \,\mu\text{m} \times$ 15 μm. Disorder is introduced by placing a low concentration of air circles (filling fraction f, radius a,  $n_{air} = 1$ ) so that  $\ell_t =$ 6.4 µm for both polarizations. Due to difference in scattering, TM/TE simulations required  $a = 100 \,\mu\text{m}$ , f = 6% and a =50  $\mu$ m, f = 5% respectively. These parameters ensured stated  $\ell_t$ , as determined from the conductance in the waveguide geometry [5]. In the remission geometry, input/output ports of width 10 µm were placed symmetrically separated by the distance 160 µm.

We simulated remission  $r_{mn}$  (for slab) and transmission  $t_{mn}$  (for waveguide) matrices, normalized so that the square of a matrix element corresponds to remitted/transmitted flux. Their eigenvalues  $\rho$  and  $\tau$  were obtained using the standard singular value decomposition procedure [1,5]. We repeated simulations to accumulate data from 1000 realizations for every system. For reference, we use previous simulations performed in Kwant for the eigenvalue distribution in the remission geometry. On the

main plot in Fig. 1, we compare the PDF of the eigenvalue  $\rho/\langle \rho \rangle$  normalized its average. The two simulations produce the same behavior quantitatively and qualitatively for both TE and TM polarizations. This confirms our previous assumption that the remission eigenvalue distribution is independent of polarization. The fact that the underlying disorder needed to obtain the same  $\ell_t$  was different in two cases, suggests that PDF of the remission eigenvalues is universal, i.e. it depends solely on  $\ell_t$  and  $\lambda$  (and not the details of disorder, or polarization). Furthermore, a MESTI simulation required  $\sim 10 \times$  less computational time compared to the equivalent Kwant simulation.

Having verified the MESTI/TE simulations, we now turn to analysis of the frequency dependence of the remission matrix. An example of such a dependence for the element  $r_{11}(\omega)$  is shown in the inset in Fig. 2. Quantitative test can be done by computing the field-field correlation function  $C_E(\Delta\omega) =$  $\langle t_{mn}(\omega)t_{mn}^*(\omega+\Delta\omega)\rangle/\langle |t_{mn}(\omega)|^2\rangle$  for the transmission and similarly for the remission geometry. The half width at half maxim (HWHM) of  $C_1 = |C_E(\Delta\omega)|^2$  is equal to 1.46D/(L +  $\ell_t \cdot \pi/2$ )<sup>2</sup>, which is related to the relaxation rate in the system [6]. Fitting MESTI/TE simulation results in the waveguide geometry to the analytical prediction [6], we determined the diffusion coefficient  $D = v\ell_t/d$ , which was impossible to directly extract from the previous CW calculation. We find that  $v = c/n_{\rm eff}$ , as expected, further verifying the correctness of our simulations. Having found the diffusion coefficient, we can now compare, with no fitting parameters, the field correlation for the remission geometry, c.f. Fig. 2. Our results demonstrate that the bandwidth of the remission correlation is also approximately equal to  $1.46D/(L + \ell_t \cdot \pi/2)^2$ . This is understandable, given that the separation between input and output ports 160 µm is on the same order as the slab thickness 200 µm. In this case, the light already reaches the output port and the opposite boundary of the slab, thus, establishing the same long-time relaxation decay rate.

# III. CONCLUSION

In this work, we demonstrated advantages of the MESTI solver for simulations of coherent remission from a large 2D disordered slab. The results are insensitive to the polarization and properly reproduce spectral features of the system. This enables future studies of the spectral and temporal behaviors of remission.

### REFERENCES

- N. Bender, A. Goetschy, C. W. Hsu, H. Yilmaz, P. Jara Palacios, A. Yamilov, H. Cao, "Coherent enhancement of optical remission in diffusive media," *PNAS* 119, 2207089119, 2022.
- [2] H. C. Lin, Z. Wang, and C. W. Hsu, "Fast multi-source nanophotonic simulations using augmented partial factorization," *Nat. Comput. Sci.* 2022, https://doi.org/10.1038/s43588-022-00370-6.
- [3] S. Gigan et al, "Roadmap on wavefront shaping and deep imaging in complex media," *J. Phys. Photonics* 4, 042501, 2022.
- [4] C. W. Groth, M. Wimmer, A. R. Akhmerov, X. Waintal, "Kwant: a software package for quantum transport," New J. Phys. 16, 063065, 2014.
- [5] N. Bender, A. Yamilov, A. Goetschy, H. Yilmaz, C. W. Hsu, H. Cao, "Depth-targeted energy deposition deep inside scattering media," *Nat. Phys.* 18, 309, 2022.
- [6] M. C. W van Rossum, and Th. M. Nieuwenhuizen, "Multiple scattering of classical waves: microscopy, mesoscopy, and diffusion," *Rev. Mod. Phys.* 71, 313, 1999.